TECHNIQUES FOR PHYSIOLOGY

Chronic imaging of cortical sensory map dynamics using a genetically encoded calcium indicator

Matthias Minderer[1], Wenrui Liu[1], Lazar T. Sumanovski[1], Sebastian Kügler[2], Fritjof Helmchen[1] and David J. Margolis[1]

[1] *Brain Research Institute, Department of Neurophysiology, University of Zurich, Switzerland*
[2] *Centre of Molecular Physiology of the Brain (CMPB) at University Medicine Göttingen, Department of Neurology, Göttingen, Germany*

Non-technical summary Optical imaging is widely used to map functional areas of the cerebral cortex. We present a method for fast fluorescence imaging of map-level cortical activity using a calcium indicator protein. Sensory-evoked neuronal activity can be imaged repeatedly in the same mouse over weeks, enabling new opportunities for the longitudinal study of cortical function and dysfunction. We hope this method will be flexibly applied across different cortical areas and to a variety of newly developed genetically encoded calcium and voltage sensors.

Abstract *In vivo* optical imaging can reveal the dynamics of large-scale cortical activity, but methods for chronic recording are limited. Here we present a technique for long-term investigation of cortical map dynamics using wide-field ratiometric fluorescence imaging of the genetically encoded calcium indicator (GECI) Yellow Cameleon 3.60. We find that wide-field GECI signals report sensory-evoked activity in anaesthetized mouse somatosensory cortex with high sensitivity and spatiotemporal precision, and furthermore, can be measured repeatedly in separate imaging sessions over multiple weeks. This method opens new possibilities for the longitudinal study of stability and plasticity of cortical sensory representations.

Introduction

Optical imaging techniques have enabled important advances in systems neuroscience by allowing investigation of spatiotemporal activity dynamics over large areas of cortex. Chronic, repeated imaging from the same subjects over long time periods is essential for longitudinal studies of cortical function, but presents additional technical challenges. While chronic imaging is well established using dye-free methods such as optical imaging of intrinsic signals (Masino & Frostig, 1996), intrinsic signals, including autofluorescence (Shibuki *et al.* 2003), have slow dynamics and an indirect relationship to

neuronal activity. Fast dynamics of cortical activity can be visualized using fluorescence imaging of organic voltage- or calcium-sensitive indicator dyes on the wide-field (WF) (Grinvald & Hildesheim, 2004; Berger *et al.* 2007) and local population levels (Grewe & Helmchen, 2009). However, organic dyes suffer from phototoxicity and non-specific staining, and critically, are not optimal for chronic experiments because they require repeated tissue staining before each imaging session (Slovin *et al.* 2002; Andermann *et al.* 2010).

Fluorescent protein indicators are well suited for chronic imaging. Genetically encoded calcium indicators (GECIs), pH- and voltage-sensitive proteins have been used for WF mapping of neuronal activity *in vivo* (Bozza *et al.* 2004; Hasan *et al.* 2004; Akemann *et al.*

M. Minderer and W. Liu contributed equally to this work.

2010), but methods have not been optimized to record fast spatiotemporal dynamics of sensory representations repeatedly in longitudinal studies. While GECIs have emerged as powerful tools for chronic two-photon imaging of action potential (AP)-related neuronal activity with cellular resolution (Mank *et al.* 2008; Tian *et al.* 2009; Andermann *et al.* 2010), their capacity for reporting large-scale cortical map dynamics has not been fully investigated.

Among GECIs, Yellow Cameleon (YC) 3.60 is a good candidate for long-term cortical mapping because it is a ratiometric FRET (fluorescence resonance energy transfer) indicator (Nagai *et al.* 2004), and therefore less influenced by optical path changes and brain motion than single wavelength indicators. Furthermore, YC3.60 expression and functional properties are stable in mouse cortical neurons over months (Andermann *et al.* 2010; Margolis *et al.* 2010), and *in vivo* cellular signals sensitively report AP firing (Lütcke *et al.* 2010). Previous studies that imaged WF GECI signals (Hasan *et al.* 2004; Lütcke *et al.* 2010) used non-ratiometric systems with limited spatial and/or temporal resolution and therefore did not capture detailed spatiotemporal activity dynamics. Chronic WF mapping of cortical activity using GECIs has not been achieved.

Here we present a method based on WF imaging of virally expressed YC3.60 for measuring fast dynamics of sensory-evoked spatiotemporal activity across large areas of mouse somatosensory cortex, using a preparation that enables long-term repeated imaging.

Methods

Animals

Experiments used male or female C57Bl6 mice, 6–10 weeks old at time of adeno-associated viral (AAV) injection, and were approved by the Zurich Cantonal Veterinary office. Presented data include 13 imaging sessions from five mice.

Viral-mediated expression

YC3.60 was expressed in neurons by intracortical injection of AAV-1/2 hybrid serotype vector AAV-1/2-hSyn-YC3.60 (2×10^8 transducing units μl^{-1}), as in previous work (Lütcke *et al.* 2010). Under isoflurane anaesthesia (4% induction, 1–2% maintenance), 100–150 nl virus mixed 1:1 with 20% D-mannitol (200–300 nl total volume) was injected through a glass pipette (5–8 μm open tip diameter) 300–500 μm below the pia at 1–3 sites into primary somatosensory cortex (mm from bregma; posterior, lateral): barrel 1 (−1, 3.3), barrel 2 (−0.8, 3.5), hindlimb (−0.5, 1.5).

Chronic cranial window

1–3 weeks after viral injection, mice were re-anaesthetized with isoflurane and implanted with a head post and cranial window. Open-skull windows (Holtmaat *et al.* 2009) used 3 mm × 3 mm no. 1 thickness square cover glass (UQG Optics or Bullen Inc.). One mouse was implanted with a polished-and-reinforced-thinned-skull window (Drew *et al.* 2010) using 5 mm no. 1 round cover glass (Menzel Gläser); data from both window types was pooled. Mice recovered for >14 days.

Histology

Mice were intracardially perfused and brains fixed in 4% paraformaldahyde. The entire cortex from the imaged hemisphere was dissected and flattened between microscope slides during post-fixation. Tangential 100 μm sections were cut on a cryotome and stained for cytochrome oxidase. Bright field images were acquired with a stereoscope and aligned to *in vivo* images in Adobe Illustrator.

Imaging setup

Our custom tandem-lens fluorescence macroscope incorporated two identical high-speed cameras (100 pixel × 100 pixel CMOS sensor; MiCam Ultima-L, Brain Vision Inc.) to visualize FRET between the cyan and yellow fluorophores of YC3.60. Fluorescence was excited through a 432 nm/25 nm excitation filter (Chroma) with a high power 60-chip 435 nm LED (±15 nm half-width; Roithner Lasertechnik) driven by a stabilized current driver (Prizmatix). Excitation light was reflected by a 50 mm dichroic mirror (Q470lp, Chroma) and focused through a 17 or 25 mm f0.95 lens (D-1795 or D-2595; Navitar). Fields of view with these lenses were 3.0 or 4.4 mm (33 or 49 μm pixel width), respectively. Cyan fluorescent protein (CFP) fluorescence emission was reflected to CMOS2 by a second dichroic mirror (DC-Blue, Linos) mounted on a kinematic platform (Thorlabs) to aid alignment, emission filtered (480 nm/40 nm; Chroma) and collected by a 50 mm f0.95 lens (D-5095; Navitar). Yellow fluorescent protein (YFP) fluorescence passed the second dichroic, an emission filter (550 nm/20 nm; Chroma), and was imaged onto CMOS1 by a second 50 mm f0.95 lens. Cameras were synchronized and acquisition controlled by MiCam Ultima imaging system (Brain Vision, Inc.).

Electrophysiology and intracortical microstimulation

Local field potential (LFP) was recorded using a glass pipette (tip diameter ∼5 μm) filled with Ringer solution (in mM: 135 NaCl, 5.4 KCl, 1 MgCl$_2$, 1.8 CaCl$_2$ and 5 Hepes) and inserted through the dura mater into layer L2/3. Signals were amplified (ELC-03XS; NPI),
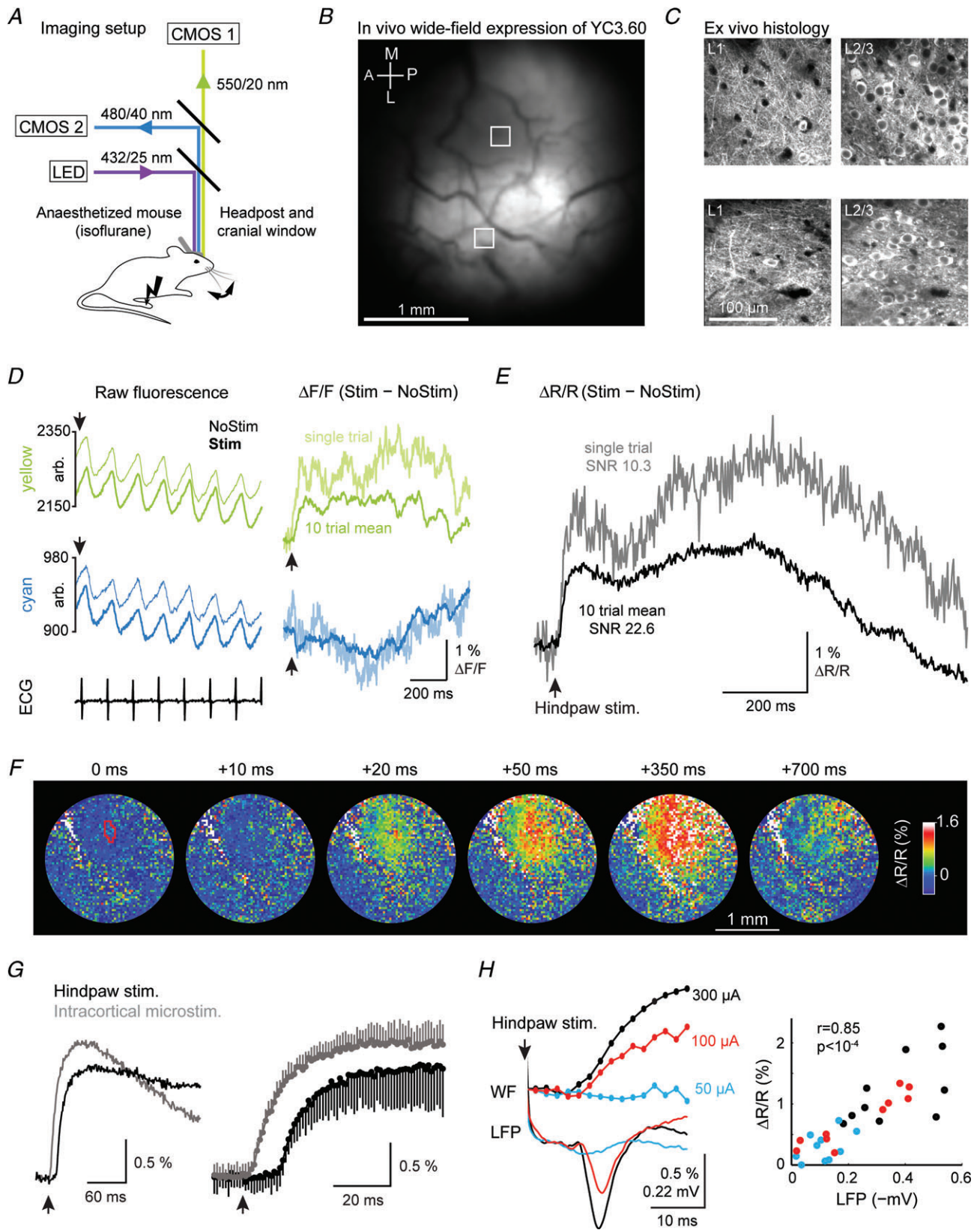
Figure 1. *In vivo* WF GECI imaging

A, schematic diagram of two-camera high-speed fluorescence imaging setup. *B*, yellow channel image of YC3.60 expression area in somatosensory cortex of an anaesthetized mouse 115 days after AAV injection. *C*,

bandpass-filtered (0.3–500 Hz), digitized at 20 kHz (ITC-18, Instrutech) and recorded using custom software (Igor Pro, Wavemetrics). Intracortical microstimulation (ICMS) current pulses from a stimulus isolator were delivered through a glass pipette (tip diameter ∼5 μm) filled with Ringer solution inserted into L2/3.

Sensory stimulation

Current pulses were delivered by a stimulus isolator to the contralateral hindpaw through a subcutaneous bipolar needle electrode. For whisker stimulation, individual whiskers were inserted into a metal tube glued to a piezo bending element (to ∼3 mm from fur) and mechanically deflected by ∼0.5 mm (∼14 degrees).

Imaging and data processing

Mice were anaesthetized with 0.5–1.5% isoflurane so that breathing rate was >1 Hz and heart rate was typically 6–10 Hz (∼350–600 beats min^{-1}). Acquisition of each trial (movie) was triggered on the electrocardiogram (ECG) using a window discriminator. To isolate stimulus-related signals, alternate heartbeat-triggered movies were acquired with (Stim) and without (NoStim) stimulation and subtracted after $\Delta R/R$ calculation. The ratiometric FRET signal (% $\Delta R/R$) was calculated as the change in (YFP:CFP) fluorescence ratio (ΔR) relative to baseline ratio (R; averaged 50–480 ms before stimulation) after detector-offset subtraction. Calcium signals are reported as % $\Delta R/R$ (Stim − NoStim) except in Fig. 1, where we show relative fluorescence changes separately for each channel ($\Delta F/F$).

Data analysis

Raw 16-bit images were analysed in ImageJ (http://rsbweb.nih.gov/ij/) using custom routines. To calculate calcium signal ($\Delta R/R$) time series, signals were spatially averaged from regions of interest (ROIs; typically containing 25–100 pixels, ∼0.03–0.1 mm^2) defined by hand or by contour level relative to signal peak. No further temporal or spatial filtering was used

for time series analysis or display. To estimate signal onset location, the first four frames (40 ms) after signal onset were averaged and spatially filtered; the signal onset location was then defined as the maximum pixel in the filtered image. Signal-to-noise ratio (SNR) was defined as the initial peak amplitude after temporal averaging (50 ms window) divided by the SD of a 50 ms pre-stimulus baseline. Decay time constants were measured from single-exponential fits.

Results

To image WF GECI signals *in vivo*, we built a macroscope using two high-speed cameras for simultaneous measurement of cyan and yellow fluorescence emission from neurons expressing YC3.60 (Fig. 1*A*; see Methods). Cortical expression areas resulting from one to three intracortical AAV injections spanned millimeters of sensory cortex and contained densely labelled neuronal somata and neuropil (Fig. 1*B* and *C*). Mice were anaesthetized with isoflurane and the cortex was imaged through a chronic cranial window. YC3.60 fluorescence signals were modulated with the heartbeat in both emission channels due to absorption by haemoglobin (e.g. Akemann *et al.* 2010), confounding the functional signals. This blood flow artifact was eliminated by triggering image acquisition on the ECG followed by subtraction of trials with and without stimulation (Stim − NoStim; see Methods) (Fig. 1*D*). After this correction procedure, we readily resolved simultaneous increases in yellow and decreases in cyan fluorescence, as expected from a FRET indicator (Fig. 1*D*, right). Single-trial ratiometric calcium signals ($\Delta R/R$) in hindlimb primary somatosensory cortex (HL) evoked by brief hindpaw stimulation (1 ms, 300 μA) could be resolved with high signal-to-noise ratio (SNR) (Fig. 1*E*). On average, SNR was 9.7 ± 6.4 for single trials and 25.3 ± 11.1 for 10-trial mean responses (mean $\pm$ SD; $n = 5$ mice, including whisker and HL stimuli). Spatiotemporal dynamics of the sensory-evoked response could be visualized at high frame rates (>500 Hz) as a localized initial response that subsequently spread over a larger area (Fig. 1*F*).

ex vivo two-photon images of YC3.60 expression in neurons and neuropil of L1 and L2/3, from same mouse as in *B* (fixed tissue; locations marked by squares). *D*: left, single trial raw fluorescence traces from each channel before (NoStim) and during (Stim) hindpaw stimulation (1 ms, 300 μA; arrows); right, single trial (thin lines) and mean (thick lines; 10 trials) $\Delta F/F$ for each channel. *E*, single trial and mean $\Delta R/R$ (10 trials) for the same data as in *D*. *F*, movie frames corresponding to the data in *D*. Red contour on first frame indicates ROI used for spatial averaging of time series. Frame rate 500 Hz in *D*–*F*. *G*: left, comparison of responses to hindpaw sensory stimulation and intracortical microstimulation (1 ms, 500 μA for each; 1000 Hz frame rate); right, same data on expanded time scale (error bars, 1 SD). *H*, simultaneously recorded LFP and WF YC3.60 signals (frame rate 500 Hz): left, mean of 10 trials at three stimulation intensities (50, 100, 300 μA); right, single-trial correlation between LFP and WF signals for 10 stimuli each at 3 different intensities, as at left (Pearson's linear correlation coefficient, $r = 0.85$; $P < 10^{-4}$). Data in *D*–*H* from the same mouse.

To measure the signal onset kinetics, we compared responses in HL cortex evoked by sensory stimulation or direct intracortical microstimulation (ICMS) imaged at 1000 Hz. While both signals rose quickly (maximum slope, mean $\pm$ SD: HL, $87 \pm 36\%$ $\Delta R/R\,\mathrm{s^{-1}}$; ICMS, $98 \pm 15\%$ $\Delta R/R\,\mathrm{s^{-1}}$; $n = 20$ trials each), the expected $\sim$10 ms difference in latency between the sensory-evoked (HL) and direct (ICMS) responses was clearly resolvable (Fig. 1G).
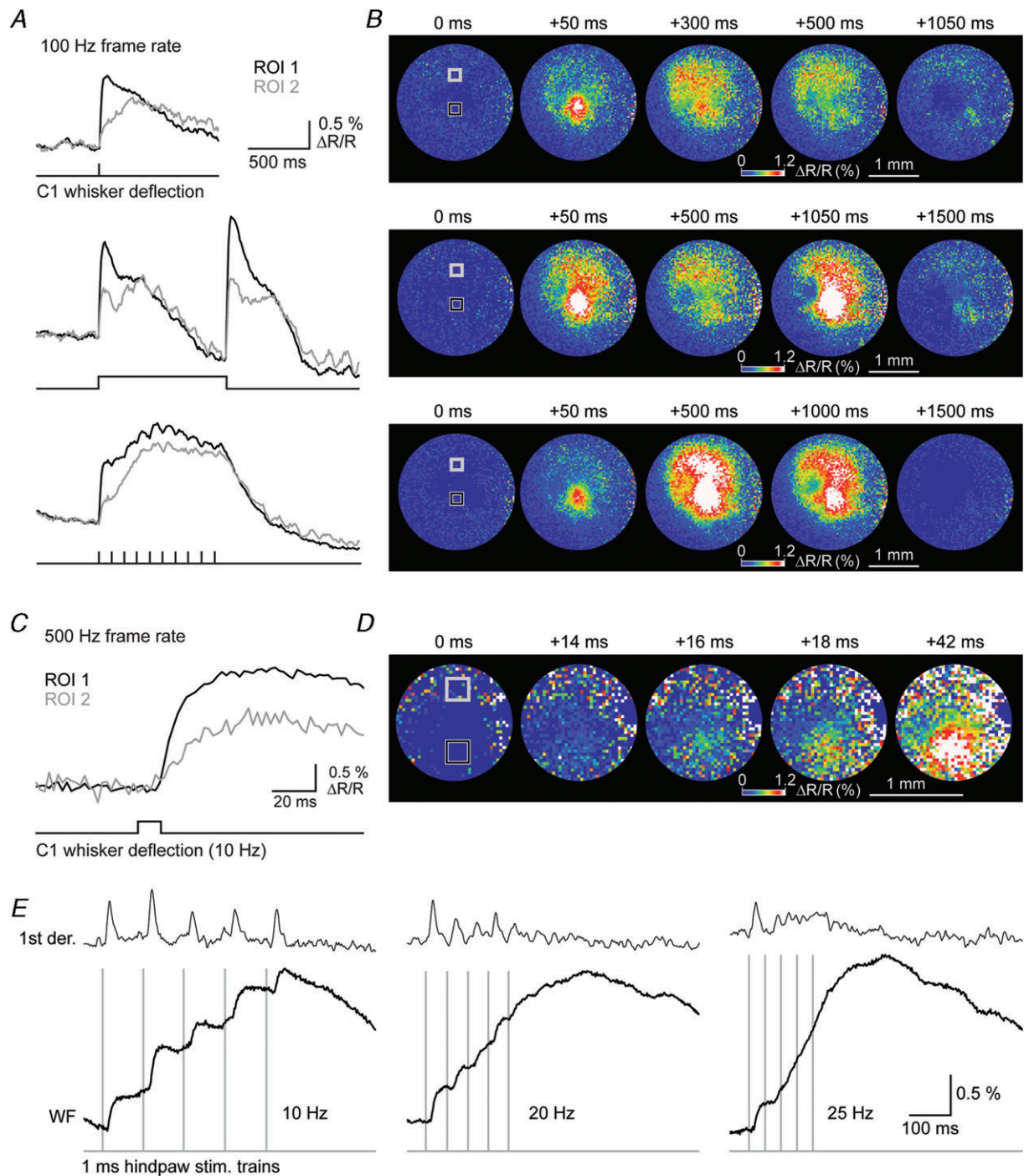
Figure 2. Sensory-evoked dynamics of WF GECI signals
A, responses in barrel cortex of one mouse evoked by three types of whisker deflections: single 10 ms (top, mean of 20 trials), 1 s step (middle, mean of 20), or 10 Hz for 1 s (bottom, mean of 40). 100 Hz frame rate. B, $\Delta R/R$ movie frames corresponding to A. Squares indicate ROI positions for data in A. C and D, signal onset imaged at 500 Hz in same session (different sweeps to those in A). E, responses in HL cortex (different mouse to that in A–D) to hindpaw stimuli of varying frequency. First derivative of smoothed WF signal shown above each trace. 500 Hz frame rate.
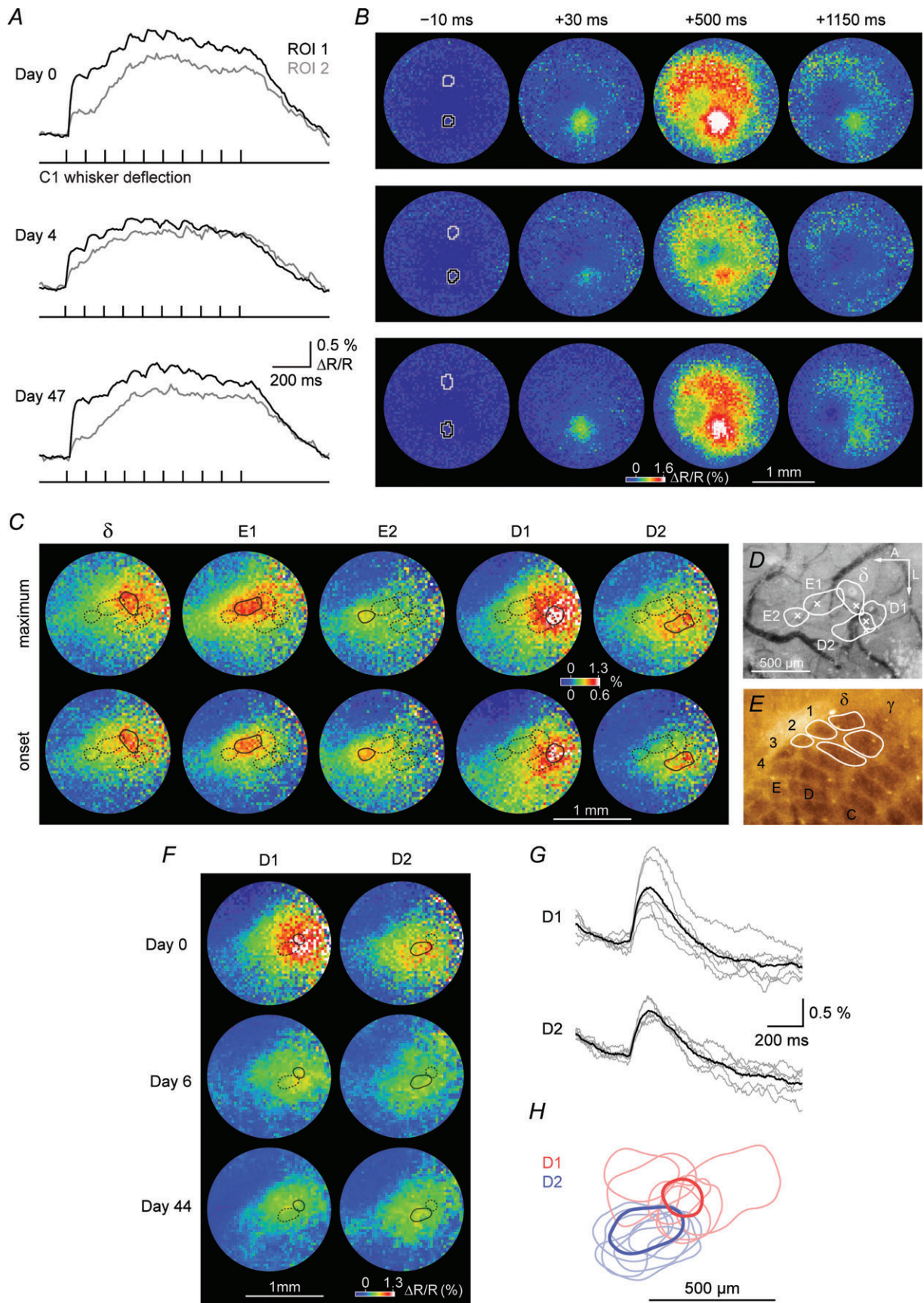
Time-to-peak from signal onset was ∼60 ms for both HL and ICMS responses (mean ± SD: HL, 58 ± 20 ms; ICMS, 57 ± 13 ms; $n = 20$ trials each). The decay time constant (τ) pooled across ICMS and whisker-evoked responses was 274 ± 27 ms (mean ± SD; $n = 20$ trials ICMS, $n = 80$ trials 10 Hz whisker stimulation). These data indicate that high-speed WF GECI imaging captures rapid cortical dynamics.

To determine the relationship of WF GECI signals to sensory-evoked neuronal activity, we made simultaneous optical and local field potential (LFP) recordings. Optical and electrical signals in response to HL stimulation of three different intensities (50, 100, 300 μA; 1 ms) on average showed close correspondence, both in peak amplitude and timing (Fig. 1H, left). Furthermore, single-trial LFP amplitude and single-trial WF signal amplitude were highly correlated ($r = 0.847$; $P < 10^{-4}$) (Fig. 1H, right), demonstrating that WF GECI signals report local electrical neural activity with high fidelity, even on the single trial basis.

The high sensitivity and SNR of WF GECI signals allowed imaging of responses to more subtle sensory stimuli. In the whisker-related barrel cortex, we compared signal dynamics evoked by different types of single-whisker stimulation, as illustrated in one example mouse (Fig. 2A and B). A 10 ms whisker deflection elicited a sharp transient with onset kinetics resembling the ICMS and HL responses of Fig. 1F (Fig. 2A, top, and Fig. 2C). During a 1 s step deflection, a clear transient was evoked at stimulus onset and, after adaptation during the holding phase, again at stimulus offset (Fig. 2A and B, middle). During a 10 Hz, 1 s train of deflections, each of the 10 transient bumps could be resolved (Fig. 2A, bottom) as well as a larger extent of spatial activation (Fig. 2B, bottom). To determine the maximum temporal resolution of WF GECI signals, we measured responses evoked by brief HL electrical stimulation at frequencies from 1 to 50 Hz (different mouse to that in A–D). Responses to individual pulses could be resolved during stimulus trains at frequencies up to 20 Hz but merged at higher frequencies (Fig. 2E), setting a practical upper limit

for imaging high-frequency sensory responses. Together, these data demonstrate the capacity of WF GECI imaging to resolve the spatiotemporal dynamics of sensory-evoked cortical activity.

To investigate spatial and temporal properties of sensory maps over time, we performed repeated imaging through chronically implanted cranial windows, allowing mice to wake up and return to their home cage between each session. As illustrated in Fig. 3A and B, the spatiotemporal dynamics of responses to 10 Hz, 1 s stimulation of whisker C1 were highly reproducible in the same mouse for up to 7 weeks. In a different mouse, we mapped five individual whiskers on one session using single 10 ms deflections (Fig. 3C). Signal contours at the 90% peak level approximated the size and position of the whisker barrels as defined by *post hoc* histology (Fig. 3C–E). Over the next 6 weeks, we tracked responses to whiskers D1 and D2 (Fig. 3F). Response amplitude and dynamics showed no degradation over time, although map position and shape as well as signal dynamics appeared more variable for the D1 than the D2 whisker, even though responses were imaged in the same sessions under identical experimental conditions (Fig. 3F, G and H). These results illustrate the use of WF GECI imaging for measuring spatiotemporal features of cortical sensory maps over a time scale of multiple weeks, and suggest the importance of longitudinal experiments for understanding long-term cortical map dynamics.

Discussion

Our data demonstrate that WF optical imaging of the GECI YC3.60 enables chronic *in vivo* investigation of the spatiotemporal dynamics of cortical activity in the anaesthetized mouse. Sensory maps can be imaged in the same mice over weeks and months, opening the possibility for longitudinal studies of stability and plasticity of large-scale cortical map dynamics.

Our method extends established cortical mapping techniques based on WF fluorescence imaging of synthetic voltage- and calcium-sensitive dyes (Grinvald

Figure 3. Long-term imaging of spatiotemporal map dynamics
A, responses in barrel cortex (mean 40 trials each) from two ROIs (indicated on first frame in *B*) to 10 Hz whisker stimulation in the same mouse imaged in three sessions over 47 days (same mouse as in Fig. 2*A* and *B*). *B*, movie frames corresponding to responses in *A*; field of view shift over days is uncorrected. Time of individual frames relative to first stimulus shown above. *C*, maximum and onset response to five individual whiskers imaged in a single session (different mouse to that in *A* and *B*). 90% contours of all whiskers are overlaid (solid line indicates stimulated whisker). Stimulus was a single 10 ms deflection; mean of 20 trials each. *D*, 90% contours overlaid on picture of blood vessels imaged through thinned-skull window (33 days after implant (49 days after virus injection). *E*, cytochrome oxidase barrel map of the same mouse (same scale as in *D*). *F*, maximum response images for whiskers D1 and D2 from three sessions over 44 days. *G*, signal dynamics and *H*, 90% contour maps of D1 and D2 whisker-evoked responses over six sessions. Thick lines indicate all-session means (also overlaid in *F*). Frame rate 100 Hz in *A–H*.

& Hildesheim, 2004; Berger *et al.* 2007) to GECIs. The key advantage is the capability to image maps with high SNR and spatiotemporal precision longitudinally without the need to re-apply the indicator. Indicator-free techniques such as intrinsic signal or autofluorescence imaging, while useful for long-term mapping experiments, lack the temporal resolution necessary to capture signal onset kinetics and high-frequency responses, as we demonstrate with WF GECI imaging. Synthetic voltage-sensitive dyes can also be used in long-term studies (Slovin *et al.* 2002), but the need for tissue re-staining makes this approach less practical. Our approach of chronic WF imaging through a cranial window preparation should also be readily applicable to other types of GECIs and recently developed probes such as genetically encoded voltage indicators (Akemann *et al.* 2010) that have so far only been used in acute experiments.

A major advantage of genetic indicators is the ability to label specific cell populations. The neuronal-specific expression we achieved using AAV-1/2 hybrid serotype with the synapsin promoter (AAV-1/2-hSyn) confines labelling to local neuron populations and avoids non-specific labelling of glia or processes of remote cells (Lütcke *et al.* 2010). In addition to neuronal somata, the neuropil (dendrites and axons) is strongly labelled (Fig. 1*C*) and gives rise to a prominent bulk signal thought to be axonal in origin (Kerr *et al.* 2005; Berger *et al.* 2007; Lütcke *et al.* 2010) that probably dominates the WF GECI signal. In this way, WF GECI imaging is more similar to fibre optic fluorescence imaging than two-photon cellular-resolution imaging (Lütcke *et al.* 2010), with the additional feature that the spread of activity can be visualized at high frame rate over large areas of cortex. Because GECIs report spiking activity rather than subthreshold membrane potential (at least at the soma and proximal dendrite) (Tian *et al.* 2009; Lütcke *et al.* 2010), and because AAV-1/2-hSyn expression labels cells primarily in L2/3 and L5 but not L4, we propose that the WF GECI signal represents population spiking activity of predominantly L2/3 pyramidal neurons. The supra-threshold nature of WF GECI signals probably explains why our whisker maps are more spatially restricted than voltage-sensitive dye signals. Maps of spiking activity will be advantageous for localizing cortical areas specifically involved in suprathreshold neuronal signal transmission.

In the future, expression could be further restricted to subtypes of neurons, such as excitatory and inhibitory cells, providing cell-specific WF activity maps. We anti-cipate that chronic WF GECI imaging of defined neuro-nal networks will provide a bridge between systems and cellular neuroscience for the longitudinal study of cortical sensory processing and plasticity in both health and disease.

References

Akemann W, Mutoh H, Perron A, Rossier J & Knopfel T (2010). Imaging brain electric signals with genetically targeted voltage-sensitive fluorescent proteins. *Nat Methods* **7**, 643–649.

Andermann ML, Kerlin AM & Reid RC (2010). Chronic cellular imaging of mouse visual cortex during operant behavior and passive viewing. *Front Cell Neurosci* **4**, 3.

Berger T, Borgdorff A, Crochet S, Neubauer FB, Lefort S, Fauvet B, Ferezou I, Carleton A, Luscher HR & Petersen CC (2007). Combined voltage and calcium epifluorescence imaging in vitro and in vivo reveals subthreshold and suprathreshold dynamics of mouse barrel cortex. *J Neurophysiol* **97**, 3751–3762.

Bozza T, McGann JP, Mombaerts P & Wachowiak M (2004). In vivo imaging of neuronal activity by targeted expression of a genetically encoded probe in the mouse. *Neuron* **42**, 9–21.

Drew PJ, Shih AY, Driscoll JD, Knutsen PM, Blinder P, Davalos D, Akassoglou K, Tsai PS & Kleinfeld D (2010). Chronic optical access through a polished and reinforced thinned skull. *Nat Methods* **7**, 981–984.

Grewe BF & Helmchen F (2009). Optical probing of neuronal ensemble activity. *Curr Opin Neurobiol* **19**, 520–529.

Grinvald A & Hildesheim R (2004). VSDI: a new era in functional imaging of cortical dynamics. *Nat Rev Neurosci* **5**, 874–885.

Hasan MT, Friedrich RW, Euler T, Larkum ME, Giese G, Both M, Duebel J, Waters J, Bujard H, Griesbeck O, Tsien RY, Nagai T, Miyawaki A & Denk W (2004). Functional fluorescent Ca^{2+} indicator proteins in transgenic mice under TET control. *PLoS Biol* **2**, e163.

Holtmaat A, Bonhoeffer T, Chow DK, Chuckowree J, De Paola V, Hofer SB, Hubener M, Keck T, Knott G, Lee WC, Mostany R, Mrsic-Flogel TD, Nedivi E, Portera-Cailliau C, Svoboda K, Trachtenberg JT & Wilbrecht L (2009). Long-term, high-resolution imaging in the mouse neocortex through a chronic cranial window. *Nat Protoc* **4**, 1128–1144.

Kerr JN, Greenberg D & Helmchen F (2005). Imaging input and output of neocortical networks *in vivo. Proc Natl Acad Sci U S A* **102**, 14063–14068.

Lütcke H, Murayama M, Hahn T, Margolis DJ, Astori S, Zum Alten Borgloh SM, Gobel W, Yang Y, Tang W, Kugler S, Sprengel R, Nagai T, Miyawaki A, Larkum ME, Helmchen F & Hasan MT (2010). Optical recording of neuronal activity with a genetically-encoded calcium indicator in anesthetized and freely moving mice. *Front Neural Circuits* **4**, 9.

Mank M, Santos AF, Direnberger S, Mrsic-Flogel TD, Hofer SB, Stein V, Hendel T, Reiff DF, Levelt C, Borst A, Bonhoeffer T, Hübener M & Griesbeck O (2008). A genetically encoded calcium indicator for chronic *in vivo* two-photon imaging. *Nat Methods* **5**, 805–811.

Margolis DJ, Lütcke H, Haiss F, Weber B, Kügler S, Hasan MT & Helmchen F (2010). Chronic two-photon calcium imaging of stability and plasticity of sensory representations in mouse barrel cortex. Program No. 377.5. 2010 Neuroscience Meeting Planner. Society for Neuroscience, San Diego, CA, USA. Online.

Masino SA & Frostig RD (1996). Quantitative long-term imaging of the functional representation of a whisker in rat barrel cortex. *Proc Natl Acad Sci U S A* **93**, 4942–4947.

Nagai T, Yamada S, Tominaga T, Ichikawa M & Miyawaki A (2004). Expanded dynamic range of fluorescent indicators for Ca^{2+} by circularly permuted yellow fluorescent proteins. *Proc Natl Acad Sci U S A* **101**, 10554–10559.

Shibuki K, Hishida R, Murakami H, Kudoh M, Kawaguchi T, Watanabe M, Watanabe S, Kouuchi T & Tanaka R (2003). Dynamic imaging of somatosensory cortical activity in the rat visualized by flavoprotein autofluorescence. *J Physiol* **549**, 919–927.

Slovin H, Arieli A, Hildesheim R & Grinvald A (2002). Long-term voltage-sensitive dye imaging reveals cortical dynamics in behaving monkeys. *J Neurophysiol* **88**, 3421–3438.

Tian L, Hires SA, Mao T, Huber D, Chiappe ME, Chalasani SH, Petreanu L, Akerboom J, McKinney SA, Schreiter ER, Bargmann CI, Jayaraman V, Svoboda K & Looger LL (2009). Imaging neural activity in worms, flies and mice with improved GCaMP calcium indicators. *Nat Methods* **6**, 875–881.

Author contributions

Acknowledgements